Research paper

Experimental investigation of agglomerate sizes of burning aluminized solid propellant

Mengying Liu*, Shipeng Li*†, Yong Wang**, Zhu Liu*, Feijuan Ma***, Xuyuan Zhou*, Xin Sui*, Rongjie Yang*, and Ningfei Wang*

*Beijing Institute of Technology, 5 South Zhongguancun Street, Haidian District, Beijing, CHINA
Phone: +86 13621300793
†Corresponding author: lsp@bit.edu.cn

**Shanghai Space Propulsion Technology Research Institute, 1777 Zhongchun Road, Minhang District, Shanghai, CHINA

***Xi'an North Huian Chemical Industries Co., Ltd, Huyi District, Xi'an, Shaanxi Province, CHINA

Received: November 8, 2017 Accepted: July 1, 2019

Abstract

The combustion of aluminized composite solid propellants is always accompanied by accumulation of oxidized aluminum particles on the reacting surface. Accurate measurement and prediction of agglomerate sizes have a significant influence on estimating two-phase flow loss of solid rocket motors, as well as calculating the infrared radiation and others. A dynamic particle size test system, which is mostly responsible for real-time particle size detection, was applied to measure agglomerate sizes during the burning of AP/HTPB compound propellants in solid rocket motor under 6 MPa. At the working stage of solid rocket motor, the Malvern Spraytec Analyzer was applied to analyze the size of agglomerate at 60 cm from nozzle outlet. Three recipes, which are no catalyst, CF (containing fluoride) contained and PF (poly fluoride) contained, for reducing the size of agglomerate were considered in this paper. Three replicates were performed under each formulation, and the results are highly reproducible. In repeated experiments of the same propellant, no significant change was detected from the measured size during the stable combustion in solid rocket motor. The presence of CF and PF leads to a decrease in the mean agglomerate sizes. Moreover, catalyst CF has a better influence on reducing the agglomerate sizes than PF. Compared with the results of literature, the test results are consistent with Hermsen and Liu model and the test system proved to be valid.

Keywords: agglomeration, aluminized propellants, size distribution, combustion

1. Introduction

In the early 1950s, the micron aluminum were considered as high-energy additive for excellent performance of propellant in increasing the specific impulse and suppressing the instability of combustion[1]. Despite the fact that, some problems have emerged, such as the loss of specific impulse in two-phase flow, more infrared radiation of plume, deposition of agglomerate in combustion chamber and so on[2]. It has been reported[3] that there will be approximately 1% I_{sp} loss for every 10% unburned aluminum. The deposition of agglomerate and combustion efficiency of aluminum are important indicators to evaluate the performance of propellant. The size distribution of aggregates during the combustion process of propellant in solid rocket motor (SRM) has a significance in evaluating and improving the formulation of propellant, estimating the specific impulse loss and calculating the feather infrared radiation of plume.

During the combustion of aluminized compound propellants, a complex chemical reaction occurs between the metal aluminum particles, the oxidant and the surrounding gas. In previous works[4], a suggestion was made that the combustion process of aluminum particles in solid propellants can be summarized as follows: concentration − sintering − detachment − agglomeration (shown in Figure 1). Many groups[5)−14)] have made

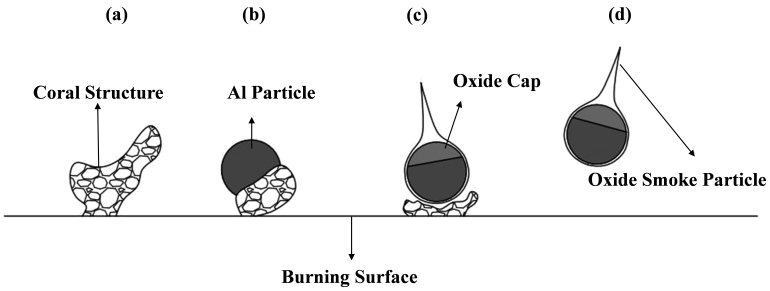

Figure 1 Combustion of aluminum on propellant surface.

outstanding contributions to the study of the combustion of aluminized propellants. Optical methods are adopted to conduct experimental studies, including videography, shadowgraphy, Schlieren, phase Doppler anemometry, and laser diffraction. Prior[15] attempts to image and size the particles during the propellant burning, but has been limited by camera focal depth. Michael[16] uses digital in-line holography (DIH) to experimentally quantify the three -dimensional position and size of aluminum during the combustion of aluminized compound propellants. Liu[17] applied cinephotomicrography technique to measure the agglomerate under 300 psi (2.07 MPa) and 1000 psi (6.89 MPa) pressures. A new agglomerate size model was also used to better explain the results of the tests. Zarko[18] used experimental methods for characterization of oxide particles formed in combustion of Al containing model solid propellants and pyrotechnic mixtures are briefly discussed.

The process of combusted propellants at room temperature and pressure or in the pressure vessel was studied by mentioned groups, but it is completely different from that in real SRM. The changes of temperature and pressure in combustion chamber will affect the combustion process of aluminum particles and the agglomeration. Collisions and further burning of alumina particles will occur when agglomerates pass through the nozzle, which will affect the size of the agglomerates. Hence, study of aggregation under actual SRM operating conditions is essential. However, due to the difficulties and limitations in experiment, almost all groups cannot directly measure the size of agglomeration in plume in the actual SRM working process.

In this paper, an advanced optical diagnostic method is adopted to measure the size distribution of agglomerates in plume during the working stage of SRM. The work begins with theoretical which helps us to understand the principles of test to be able to analyze the rationality of test. Then, the experimental arrangement is shown. In order to ensure the same pressure in the combustion chamber of the motor, the burning rate of the propellants in different formulations was measured for designing the SRM, and the dynamic particle size test is followed. Experimental results are then compared with the results from the literature and models, which help to validate the proposed measurement techniques.

2. Theoretical

When laser irradiating onto the surface of particles, the surface will produce interference effects, resulting in scattering spectra[19]. The conversion from scatter gram to particle size distribution includes three steps: Firstly, the coherent laser is emitted by the laser source and hits the sample particles, scattering occurs on the particle surface. Then, the scattered light emitted by the surface of particles is captured by the photodetector, and the information of the diffracted light is converted into a digital signal. Lastly, the digital signal is deconvoluted through the appropriate instrumentation and the particle size distribution is formed.

The angle of scattered light is inversely proportional to the diameter of sample particle and to be more specific, the intensity of the scattered light decreases logarithmically as the angle of scattered light increases[20]. Based on this principle, Malvern Spraytec Analyzer analyze the size distribution of sample particles.

At present, Fraunhofer diffraction and Mie scattering theory are commonly used in predicting the absorbed and emitted light by particles. When Fraunhofer diffraction theory is used, only the refraction of light is considered, irrespective of the absorption and refraction of light by particles. Thus, when the particle size d is larger than 4λ (λ is the wavelength of incident wave), the theoretical results will be more reliable. When the particle size d is smaller than 4λ, the distribution of the scattered light is wide, so the absorption and refraction of light by particles must be considered and the Mie scattering theory is more reliable.

Assuming that the measured particle is spherical or nearly spherical in shape, scattered light consists of three parts: diffracted light, refracted light and reflected light. The ratio of absorption and scattering was determined by optical properties of particles, refractive index, size of particles and environmental medium. For the test equipment used in this paper, the wavelength of laser is 670 nm, and scattering angle at the energy peak of scattering light is θ_{max}:

$$\lambda\theta_{max} = 1.357$$

Where λ is the wavelength of the incident wave. It is noteworthy that the diameter of particles reaching Rayleigh limit, which means the diameter of particles approaching the wavelength of laser, the approximate relationship does not hold and needs to be corrected.

Spraytec[21] is a particle size analyzer from Malvern Company, which has the advantages of fast test and no destructive test sample. In this paper, Sprayte was used to

Table 1 Propellant formulations.

	Al [wt%]	HTPB [wt%]	AP [wt%]	Catalyst CF [parts]	Catalyst PF [parts]	Al^0 [μm]
P0	18	12	70	0	0	20
P1	18	12	67	0	3	20
P2	18	12	67	3	0	20

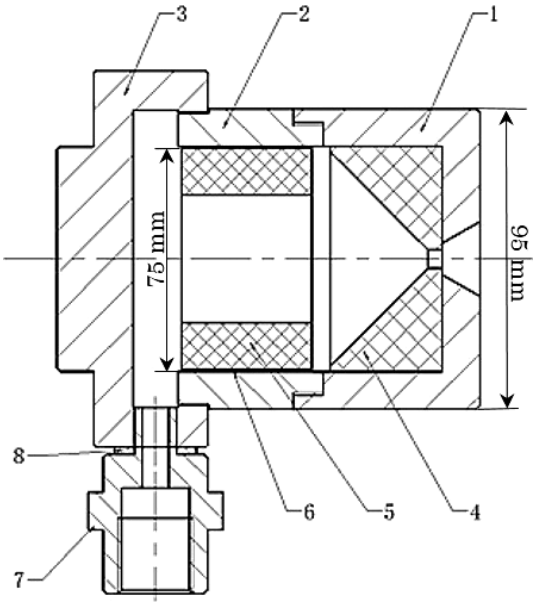

Figure 2 The structure of experimental solid rocket motor. 1: nozzle case; 2: chamber case; 3: rear dome; 4: nozzle; 5: propellant; 6: thermal barrier; 7: sensor adapter 8: shim.

analyze the size of agglomeration during the work stage of SRM. The test frequency is 1 kHz and the measuring range is 0.287 − 1000 μm.

3. Experimental equipment

Based on Malvern Spraytec Analyzer, an advanced and improved system was presented to obtain the size distribution during the burning of considered propellants in SRM.

3.1 Experimental solid rocket motor

The addition of a certain catalyst to the aluminized compound propellant can effectively improve the combustion efficiency of the propellant and reduce the particle size of the propellant in the combustion process, thereby improving the overall performance of the propellant[22]. With the decrease of the size of agglomeration, the deposition during the motor work process will be reduced accordingly, which will greatly improve the performance of solid rocket motors. In this paper, three HTPB components propellants (named P) have been subject of investigation. Laboratory-made catalyst PF (poly fluoride) and CF (containing fluoride) were added into the formulation as a comparison. The components of PF and CF are still under study, and the relevant results are not yet mature. Some previous research on the mechanism of reducing the agglomerate can be seen in the works of Zhou et al.[22] and the detailed results will be further published. As the reference, the fluorinated hydrocarbon released by the catalyst can efficiently reduce the deposition of Al_2O_3 on the surface of the aluminum-burning particles, as well as the aggregation of aluminum on the combustion surface. All propellants in this experiment were prepared by our partner laboratory and the formulation was the same as that in Zhou et al.[22] The content of aluminum in the propellant was 18%, and the virgin size of aluminum particles was 20 μm. The propellants without catalyst were coded P0 and those adding PF / CF were coded P1 / P2. Table 1 describes the propellant formulations used in this paper.

Table 2 throat diameter of each propellant.

Propellant	P0	P1	P2
Throat diameter [mm]	10.7	11	10.8

A series of standard 75 mm SRM were used, which have axisymmetric structures. The inner diameter of SRM was 75 mm and the wall thickness of combustion chamber was 10 mm, as shown in Figure 2. The design pressure in combustion chamber during the stable working stage was 6 MPa. When the propellant changed, only the diameters of throat needed to be changed, as shown in Table 2. The mass of propellant in each motor was 0.4 kg. To simulate the actual work process of SRM, the internal combustion and free filling form of propellant was adopted. The propellant in SRM was ignited by black powder, which was the same as the conventional ignition method. Besides, the mass of black powder was 25 g in each motor. The pressure sensor adapter was connected between the combustion chamber and the rear dome to measure the pressure in combustion chamber during the work of SRM. The pressure sensor model was ZQ-Y3. Rear dome and thrust sensor was connected and the thrust sensor model was CT15.

3.2 Dynamic particle size test device

In previous work of our labortary[23], the initial size distribution of agglomerate during the combustion of aluminized compound propellants at room temperature and pressure was successfully measured by the Malvern Spraytec Analyzer. Based on our previous works, a new type of dynamic optical test system for size distribution of agglomeration in plume during the motor operation was established. Compared with room temperature and pressure, agglomeration in the plume have higher temperature and brightness, which greatly increase the difficulty in measuring the size of particles by Malvern Spraytec Analyzer. In order to solve this problem, we have considered several approaches, such as adding a

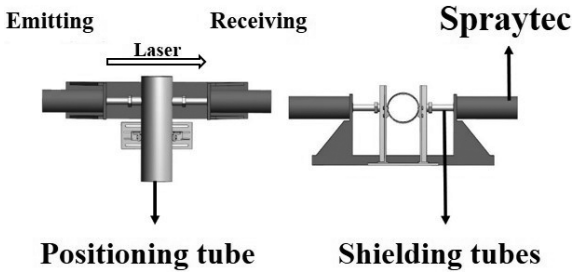

(a) Malvern Spraytec Analyzer test system.

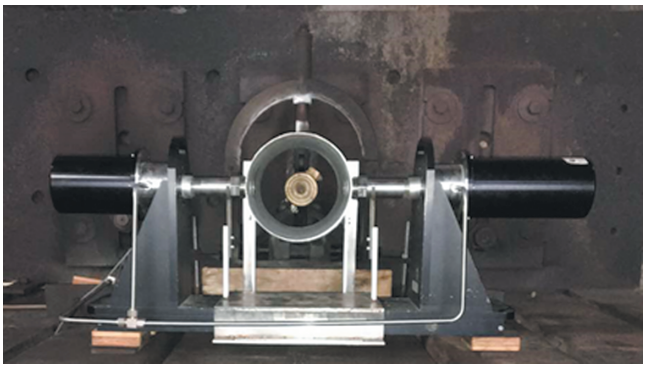

(b) Actual dynamic size test equipment.

Figure 3 Dynamic particle size measurement.

filter to the laser receiving end of Malvern Spraytec Analyzer to reduce the brightness of the measured particles, where no changes were detected. After a series of tests, the measurement devices, as shown in Figure 3, was finally adopted which mainly consist of a Malvern Spraytec Analyzer, a protection system, a data acquisition card, a processing system, a SRM, a positioning tube and two shielding tubes. The positioning tube and shielding tubes were designed to reduce environmental light interference during the test. Two symmetrical through-holes were distributed at the side of the positioning tube. Both of the shielding tubes with smaller diameter were connected to positioning tube by the through-holes, and the laser beam passed through the tubes from the laser emitting end to the receiving end to obtain the size distribution of particles in the plume. In addition, the diameter of the position tube should to be large enough in order not to interfere with the gas flow of the SRM. At the beginning of the test, it is necessary to ensure that the central axis of the motor, the axis of the positioning tube, and the laser beam are in the same plane.

4. Results and discussion

For N measured particles, D_{pq} are the mean diameters defined as,

$$D_{pq} = \left(\sum D_i^p / \sum D_i^q\right)^{\frac{1}{p-q}}$$

In this paper, $D_v(50)$ is used to illustrate the mean diameter of agglomeration, and it's expression is,

$$D_v(50) = \sqrt[5]{\left(\sum D_i^5\right)}$$

In order to compare the results of each experiment, a

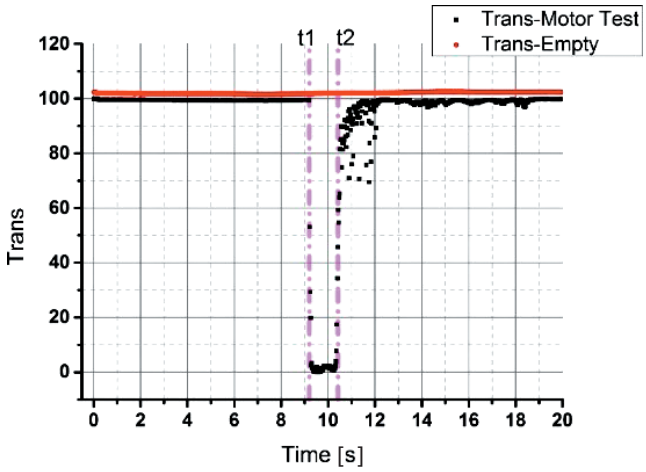

Figure 4 Transmittance of SRM and blank test.

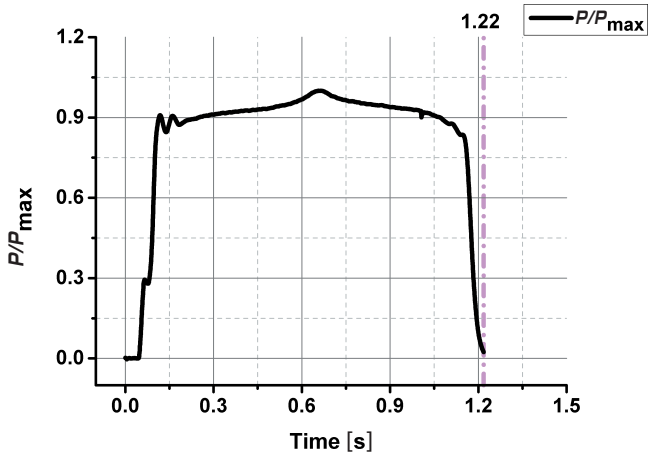

Figure 5 The working stage of SRM.

blank test with the motor no working was performed prior to SRM test. Taking one of the tests as an example, a comparison of the transmissivity signals of the blank test and the SRM test is shown in Figure 4. It reveals that the transmittance was kept at 100 in the blank test, indicating that no feather particles passed through the laser beam. From the beginning of the test until t_1, the transmittance was the same as that of the blank experiment, which remained at 100. However, the transmittance rapidly decreased to 6.1 after t_1, and the transmittance increased to 100 after t_2, returning to the same level as the blank test. Therefore, the t_1–t_2 period, which is about 1.22 s, was considered as the working time of SRM. Temporarily, the period t_1–t_2 of the decrease of the transmittance coincides with the duration of the entire SRM operation determined by the pressure curve shown in Figure 5. It shows that agglomerated particles in the plume obscure the laser beam and result in changes in the transmitted signal. Thus, the optical test system proves to be useful in measuring particle size distribution in the plumes. The transmissivity signal shows significant fluctuations after SRM operation, which mainly due to the irregular flow of residual particles in the shielding tube.

The performance parameters of propellants P0, P1 and P2 were obtained experimentally, as shown in Table 3. These propellants have similar chemical compositions, but differ in their content of catalyst. And the results show

Table 3 Performance of SRM in tests.

Propellant	P0	P1	P2
D_v (50) mean value at working stage [μm]	105.47	86.74	88.5
D_v (50) standard deviation at working stage	28.79	22.47	32.03
Particle size of SEM [μm]	5.94	3.67	2.70
Burning time [s]	1.09	1.20	1.17
Burning rate [mm/s]	9.21	8.37	8.56
Specific impulse of SRM [s]	235.10	231.16	230.60
Specific impulse efficiency [%]	89.72	89.55	88.62

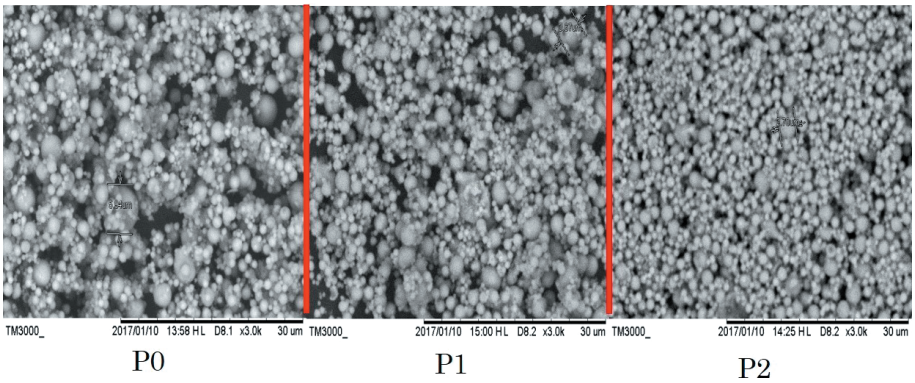

Figure 6 Scanning electron microscope (SEM) of collected deposition of propellant P0, P1 and P2 after combustion in SRM.

that the presence of catalyst has a significant effect on the size distribution. The size of the agglomeration in the plumes of propellants P1 and P2 with addition of catalyst PF and CF were obviously smaller than that of propellant P0 without catalyst addition. The addition of PF / CF reduced D_v (50) from 105.47 μm to 86.74 μm / 88.5 μm at stable working stage.

The process of aluminum on the burning surface is: igniting and melting − moving and concentrating (agglomeration) − leaving the burning surface - further burning in the flame. After leaving the burning surface, part of alumina formed by the combustion of aluminum dissipates with the hot gas, and others is deposited on the surface of burning aluminum particles. Then, the deposition of alumina coats the entire surface of aluminum particles and eventually blocks the reaction. Therefore, the size of molten aluminum leaving burning surface greatly determines that in the flame and the final agglomeration product[18].

Propellants containing catalysts PF and CF produce large amounts of fluorinated hydrocarbon gases during the combustion, as well as carbonaceous. On one hand, the fluorinated hydrocarbon gas promotes the molten aluminum away from the burning surface, which reduces the probability of collision and fusion, and inhibits the formation of larger-sized molten aluminum in the burning surface. On the other hand, according to the past studies[24),25], the fluorinated hydrocarbons are extremely reactive, which can accelerate the reaction of further burning in the flame to form oxides ($A1_2O_3$) and fluorides ($A1F_3$). The $A1F_3$ has a lower boiling point and is easily vaporized from the surface of aluminum particles at high temperatures, which results in part of $A1_2O_3$ can be taken away. Thereby, the deposition of $A1_2O_3$ on the surface of aluminum particles is reduced, as well as the decrease of the agglomeration size. However, according to the previous work[26], the addition of PF and CF results in the slightly decrease of burning rate, as is shown in Table 3.

Figure 6 is an enlarged view of the collected agglomeration of propellant P0, P1, and P2 in combustion chamber after SRM tests by scanning electron microscopy (SEM). The addition of catalyst makes the particle size of the agglomeration decrease greatly after the propellant is burned, and the accuracy of dynamic particle size measurement is verified. However, the results of dynamic particle size measurement are more larger than that of SEM in combustion chamber, as shown in Table 3. The agglomeration with smaller size in the plume are distributed at the edge of plume, due to smaller inertial force, which contributes to diffusing together with gas and changing their own trajectory more easily. In addition, the deposition in the combustion chamber does not experience collisions in the nozzle and further combustion in the plume. However, the flow of particles in nozzle during the work of motor was difficult to analyze and measure, so the specific reasons are needed for further exploration. Apart from this, the results of SEM show the same trend as the test results in reducing of agglomeration size between P0, P1 and P2.

To verify the repeatability of the test, three replicates were carried out under each formulation. The results of the tests for propellants P0, P1 and P2 are shown in the Figure 7, from which better repeatability can be seen. The pink dotted line in the figure is the actual working time of the motor determined by tested the pressure curve. However, since the flow of agglomeration was delayed in the motor, the working time in Figure 7 was slightly longer than that in Table 3 which was determined by

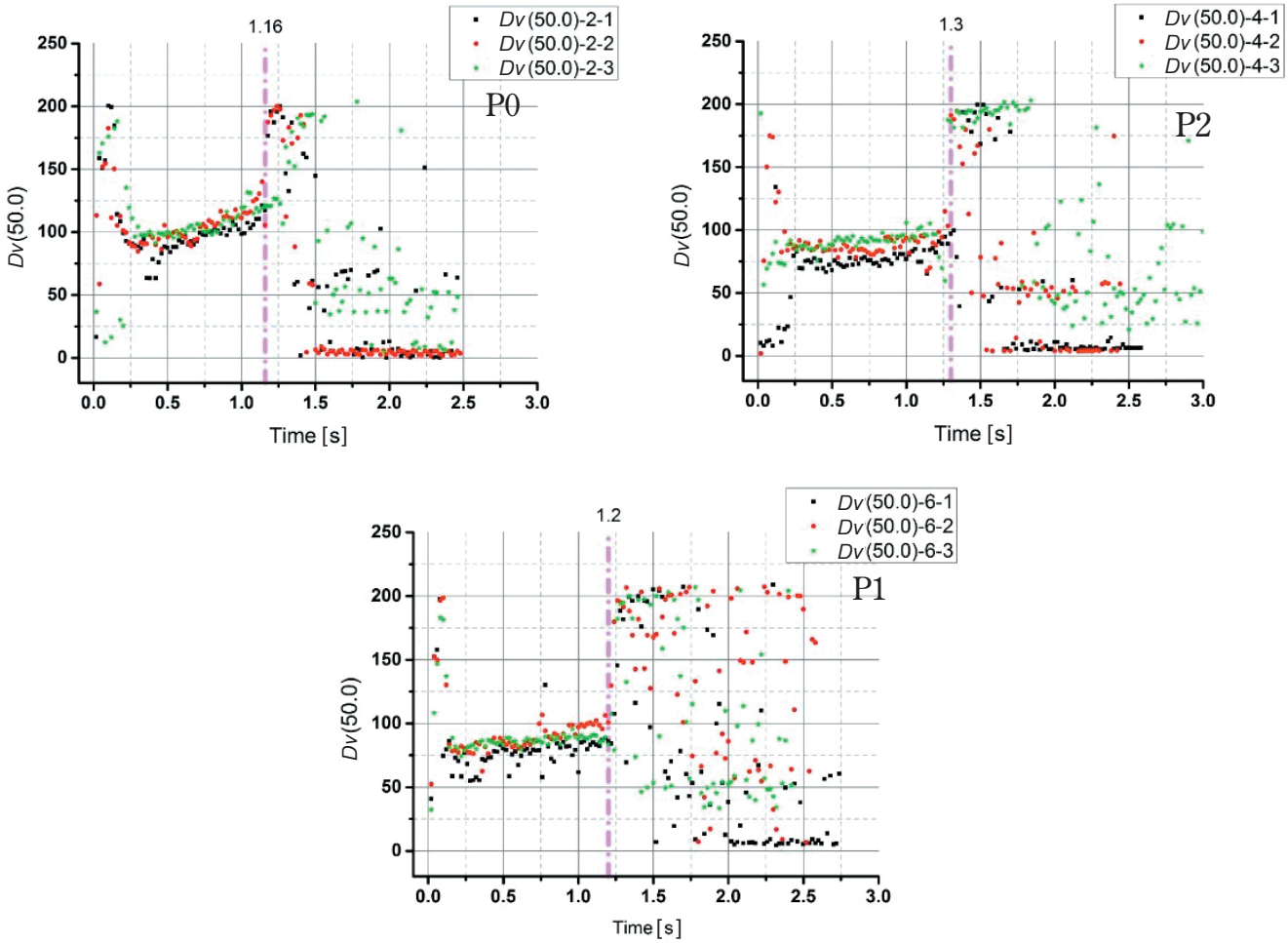

Figure 7 Size distribution of aggregation in plume of three component propellants P0, P1, and P2.

pressure curve. At the beginning of working stage, the particle size measured by the experiment was not uniform, mainly due to the influence of the black powder used in ignition. In the stable working stage of the motor, the experimental data of the three groups appeared high repeatability in all condition, which proved the feasibility and correctness of the test method. When the motor stopped working, the results were uncertain and irregular in that the particles measured the residual smoke remained in the positioning tube after combustion.

For P0, P1 and P2, the addition of PF and CF results in the reduction of the plume particles size by about 15 μm. Compared with the catalyst CF, the catalyst PF has a greater effect on reducing the size of agglomeration. However, it is worth noting that the specific impulse of SRM has no obvious effect due to the presence of PF and CF. And the specific impulse was calculated from the thrust curve measured by SRM in 3.3.

In order to verify the accuracy of the test results, Hermsen model[27] and Liu Model[17] are used to compare the experimental results of the experiment. Hermsen modelis the most classic theoretical model in literature and is used widely. Based on this, Liu has made some improvements by means of experiments and introduced the relevant variables, such as initial aluminum particle content, particle size and burning rate into the model.

Table 4 D_{ag} of theoretical models and SRM tests.

	Hermsen model [μm]	Liu model [μm]	SRM test [μm]
P0	137.74	72.06	105.47
P1	158.30	82.85	86.74
P2	155.01	81.03	88.5

Hermsen Model

D_{ag} = 35 [μm]/(AP mass fraction × burning rate [in./s])

Liu Model

D_{ag} = (2690 [μm](wt% of AP+wt% of cyclic nitranmine+1) {[wt% of AP + wt% of cyclic nitranmine] × r_b [mm s^{-1}] × [D_{Al}^0 [μm]/50 + 1]}

Table 4 lists the results of the three component propellant calculated by Hermsem and Liu models and the results measured in this experiment. Liu has a significant effect on the model correction, and the test results show good agreement with the Hermsen and Liu models. On the other hand, it also reveals the correctness of the tests.

Through the holographic method, Liu[17] obtained the particle size distribution of agglomeration during the combustion of propellants under high pressure, and found that the pressure has a significant effect on the size of the particles, shown in Figure 8. The size of the agglomeration

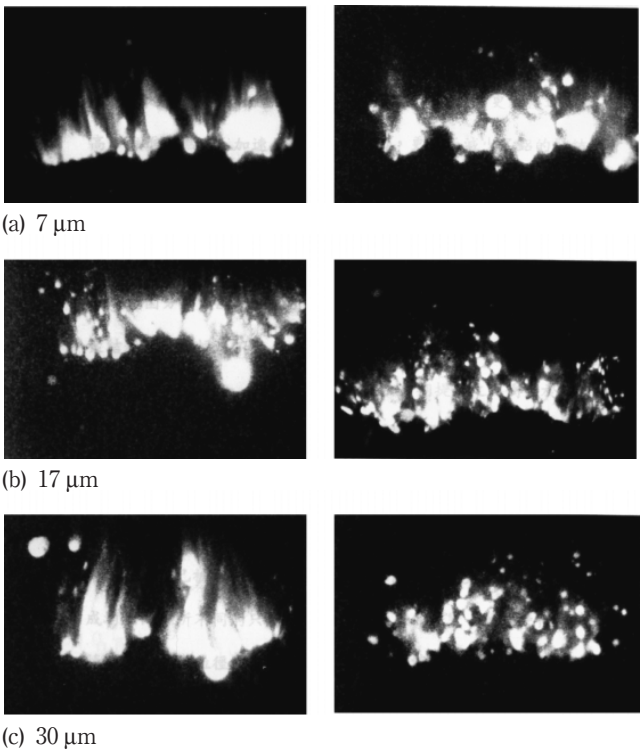

(a) 7 μm

(b) 17 μm

(c) 30 μm

Figure 8 Image results by Liu.

will decrease as the pressure increases. Oide[28] also reveals that the relation between agglomerate diameter and burning rate of propellants is obtained. Agglomerate diameter decreases with increasing burning rate. And it is expected that agglomerate diameter decreases with decreasing stay time of Al particle at burning surface.

We fitted all the available data from the experiment and obtained the size distribution of Agglomeration under different pressures which is shown in Figure 9. In the figure, the size of aggregation of all propellants varies with pressure and follows a linear correlation, which coincides with the experimental result of Liu[17]. However, due to the lack of experimental data, we cannot draw the corresponding conclusion, and further exploration is also needed.

5. Conclusion

The considerable process has been achieved in the development of the experimental techniques designed for investigating size distribution of the agglomerate particles. The advanced and improved system, based on a laser diffraction technique, provides an effective tool for studying particles size distribution of propellants in solid rocket motor. Three formulations (P0, P1, P2) were subjected to motor ignition tests and the pressure in the

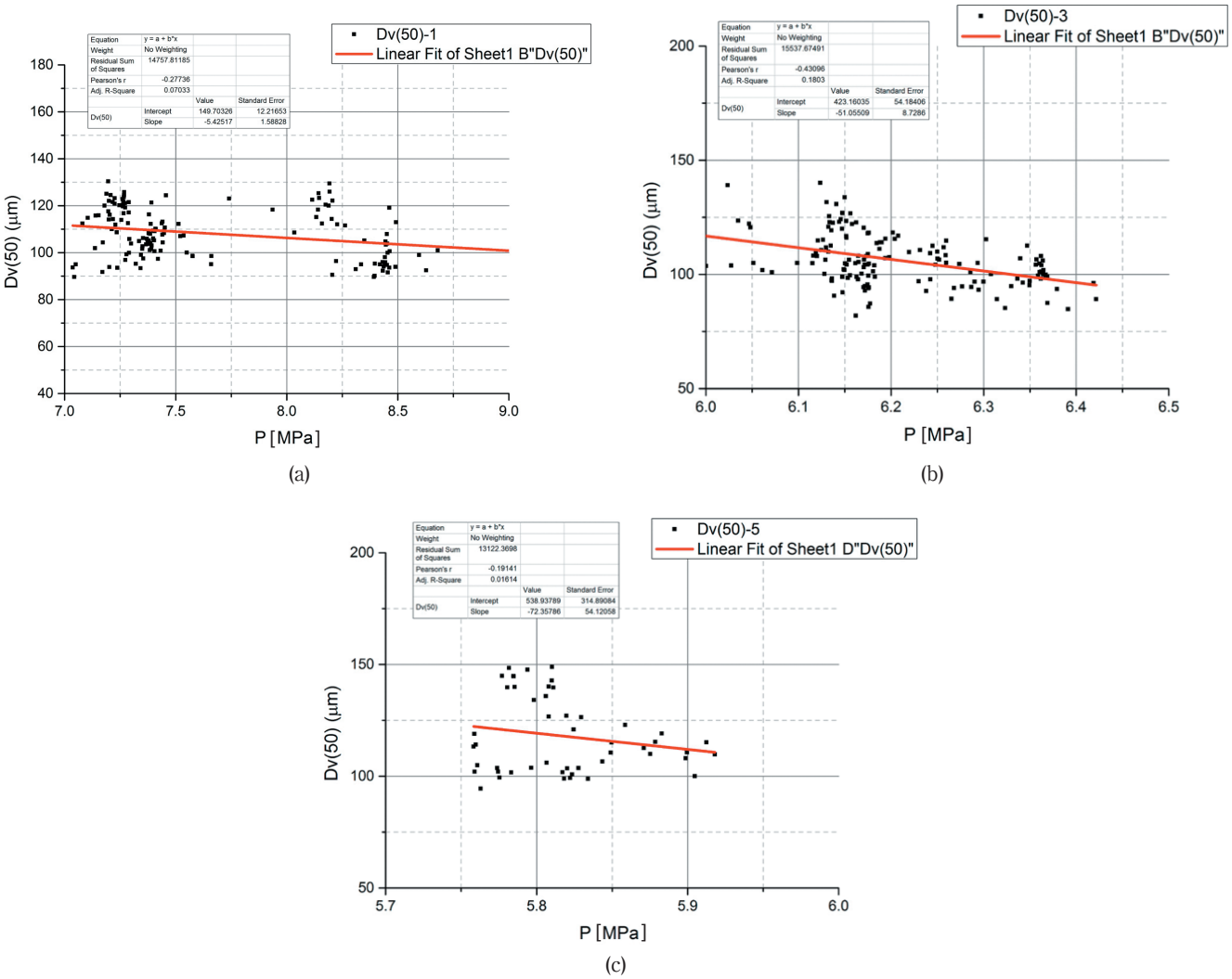

Figure 9 $D_v(50)$ variation under different pressure conditions.

combustion chamber was 6 MPa. Meanwhile, the size distribution of agglomeration in the plume at 60 cm from nozzle outlet was obtained. The results reveal that the addition of catalysts PF and CF has a significant effect on reducing the size of particles, but does not reduce the specific impulse of SRM. In addition, compared with the results of Hermsen Model and Liu Model, it is found that the test results proved to be valid. In summary, the system provides an approach for subsequent theoretical research on prediction of particle size in the plume during the work of SRM and evaluation of propellant formula more accurately.

Reference

1) K. Takahashi, K. Nakadai, S. Oide, M. Tanabe, T. Kuwahara, and T. Shimada, Sci. Tech. Energetic Materials, 74, 144−152 (2013).
2) A. B. Vorozhtsov, Sci. Tech. Energetic Materials, 76, 105−109 (2015).
3) M. L. Hartman, Chem. Propuls. Infor. Agency Bull. 24, 1−12 (1998).
4) L. T. Deluca and F. Severini, L. Nov. Energ. Mater. Appl., paper 18, 1−18 (2004).
5) D. S. Sundaram, P. Puri, and V. Yang, Combust. Flame, 169, 94−109 (2016).
6) D. Laredo, Mccrorie, J. K. Vaughn, and D.W. Netzer, J. Propuls. Power, 10, 410−418 (2012).
7) R. A. Dobbins and L. D. Strand, AIAA Journal, 8, 1544−1550 (1969).
8) Y. Feng, Z. Xia, L. Huang, and X. Yan, Acta Astronautica, 129, 1−7 (2016).
9) X. Liu, P. J. Liu, and B. Jin, 51st AIAA/SAE/ASEE Joint Propulsion Conference, 10.2514 / 6.2015-3977, AIAA Propulsion and Energy Forum, Orlando (2015).
10) T. R. Sippel, S. F. Steven, and L. J. Groven, Combust. Flame, 161, 311−321 (2014).
11) W. Pang, L.T. Deluca, X. Fan, F. Maggi, H. Xu, W. Xie, and X. Shi, Combust., Sci. Technol., 188, 315−328 (2016).
12) J. C. Mullen and M. Q. Brewster, 44th AIAA/ASME/SAE/ASEE Joint Propulsion Conference and Exhibition, 2008−5259, Hartford (2008).
13) V. A. Babuk, V. A. Vasilyev, and M. S. Malakhov, J. Propuls. Power, 15, 783−793 (2012).
14) T. K. Liu, H. Perng, S. Luh, and F. Liu, J. Propuls. Power, 8, 1177−1184 (1992).
15) J. C., Melcher, H. Krier, and R. L. Burton, J. Propuls. Power, 18, 631−640 (2002).
16) M. S. Powell, I. W. Gunduz, W. Shang, J. Chen, S. F. Son, Y. Chen, and D. R, Guildenbecher, J. Propuls. Power, 34, 1002−1014 (2018).
17) T. K. Liu, J. Propuls. Power, 21, 797−806 (2005).
18) V. E. Zarko and O. G. Glotov, Sci. Tech. Energetic Materials, 74, 139−143 (2013).
19) B Scarlett, Am. Pharm. Rev, 6, 93−101 (2003).
20) International Standards Organization (ISO) 1999. Particle Size Analysis-Laser Diffraction Methods: Part 1: General Principles. ISO, Geneva, Switzerland.
21) Malvern Spraytec particle size analyzer, https://www.malvernpanalytical.com.cn, (accessed: 21 October 2016). (online).
22) X. Zhou, M. Zou, F. Huang, R. Yang, and X. Guo. Prop., Explos., Pyrotech., 42, 417−422 (2017).
23) Z. Liu, S. Li, M. Liu, D. Guan, X. Sui, and N. Wang. Acta Astronautica, 133, 136−144 (2017).
24) M. A. Hobosyan, K. G. Kirakosyan, S. L. Kharatyan, B. K. S. Martirosyan, J. Therm. Anal. Calorim., 119, 245−251 (2015).
25) M. Losada and S. Chaudhuri, J. Phys. Chem. A, 113, 5933−5941 (2009).
26) X. Zhou, F. Huang, R. Yang, M. Zou, D. Guan, and S. Li, J. Astronautics, 38, 310−316 (2017).
27) R. W. Hermsen, 19th Aerospace Sciences Meeting, 6, 1981−1938, Aerospace Sciences Meetings, St. Louis (1981).
28) S. Oide, K. Takahashi, and T. Kuwahara., Sci. Tech. Energetic Materials, 73, 153−156 (2012).